JOURNAL OF MATERIALS SCIENCE 27 (1992) 1250–1254

Thermoelectric properties of fine grained (75% Sb_2Te_3–25% Bi_2Te_3) *p*-type and (90% Bi_2Te_3–5% Sb_2Te_3–5% Sb_2Se_3) *n*-type alloys

F. A. A. AMIN, A. S. S. AL-GHAFFARI, M. A. A. ISSA, A. M. HASSIB
Materials Group, Department of Physics, Faculty of Science, King Saud University, PO Box 2455, Riyadh 11451, Saudi Arabia

The thermoelectric properties of fine-grained alloys prepared by either cold pressing and sintering or hot pressing in the range 5–50 μm are compared with single-crystal best-direction values. It is shown that for the *p*-type alloy, almost the entire thermoelectric properties are recovered, i.e. the figure of merit for the finest grain size is almost the same as the best single-crystal value. The same trend is observed in the *n*-type alloy except that 90% of the single-crystal figure of merit is recovered. These results are discussed in terms of a model which suggests that degradation of favourable thermoelectric properties by powdering the alloys is compensated by (1) decrease of thermal conductivity due to scattering of phonons at grain boundaries for grain sizes that are comparable to the mean free path of phonons; and (2) retention of some of the anisotropic properties of the single crystal in the fine-grained compacts.

1. Introduction

One of the best thermoelectric materials for use near room temperature is Bi_2Te_3. The establishment of this material goes back to the work of Goldsmid and Douglas [1]. The early work of Ioffe [2] indicated that solid-solution alloying would be effective in scattering phonons but not electrons and would thus result in improving the figure of merit, Z. The work of Ioffe seems to have led to a considerable effort and consequently a group of solid solutions based on $(Bi, Sb)_2(Te, Se)_3$ was developed [3–6]. The review by Yim and Rosi [7], gives a systematic survey of the thermoelectric properties of compound tellurides and their solid solutions. The best *p*-type materials seem to be the Sb_2Te_3-rich solid solutions and the best *n*-type materials are the Bi_2Te_3-rich solid solutions [8] which have an average figure of merit in excess of $3 \times 10^{-3}\,K^{-1}$ at room temperature.

Bi_2Te_3 and its associated solid solution are hexagonal anisotropic materials with the figure of merit largest along the (1 1 1) plane [9]. The electrical conductivity of Bi_2Te_3 is some three to four times larger along the (1 1 1) plane than normal to it, while the thermal conductivity is much less dependent on anisotropy, being twice as large in a direction parallel to the (1 1 1) plane as a direction perpendicular to it. The Seebeck coefficient is nearly equal along the various directions. The figure of merit usually quoted for Bi_2Te_3 and its solid solution is highest in a direction parallel to the (1 1 1) plane.

The improvement in the figure of merit, Z, caused by solid-solution alloying is due to scattering of phonons, caused by the disorder in the lattice due to alloying, and thus other types of disorder, e.g. point defects, dislocations, stacking faults, line defects and grain boundaries, can also increase the figure of merit. The reduction of thermal conductivity by grain-boundary scattering of long wavelength phonons is well established for isotropic Ge–Si alloys [10] where it is always expected that Z will be improved on obtaining grains that are small enough for the onset of phonon scattering, but theoretically the same treatment cannot be applied to Bi_2Te_3-based alloys because their figure of merit is highest parallel to the (1 1 1) plane. Therefore, fine-grained Bi_2Te_3 alloys are expected to have degraded thermoelectric characteristics due to the loss of preferred orientation. The object of this work was to determine the net effect on thermoelectric properties resulting from loss of preferred orientation and reduction of thermal conductivity caused by phonon scattering at grain boundaries.

2. Experimental procedure

2.1. Alloy preparation

Two alloys were selected for the present study, both of which have a high figure of merit. The *p*-type alloy chosen was the 75% mol Sb_2Te_3, 25% mol Bi_2Te_3, $(Bi_{0.25}$–$Sb_{0.75})_2Te_3$. The *n*-type alloy was the 90% mol Bi_2Te_3, 5% mol Sb_2Te_3 and 5% mol Sb_2Se_3 $(Bi_{0.9}$–$Sb_{0.05})_2$ $(Te_{0.95}$–$Se_{0.05})_3$. The *p*-type alloy was doped with selenium to a resistivity value of (0.2 Ωm) and the *n*-type alloy doped with SbI_3 to a resistivity value of (0.3 Ωm).

The starting elemental materials were tellurium, selenium (specpure), bismuth and antimony (Analar

0022–2461

grade reagent). The bismuth and antimony were given a refining treatment before use consisting of first vacuum melting to remove any volatiles followed by zone refining. Single crystals were grown using Bridgman techniques. Prior to crystal growth, appropriate weight fraction of the elements to give the desired alloy together with the dopant were melted inside evacuated silica tubes of 1.2 cm internal diameter using resistance heated furnace. The molten charge is usually maintained molten for a period of 12 h with frequent mechanical agitation. For the Bridgman method, a drop rate of 1 cm h^{-1} was employed. R.f. power was used for melting and the furnace had a temperature gradient of 25 K cm^{-1}.

2.2. Hot pressing and sintering

The single-crystal rods were first broken down into small grains ($L \leqslant 2 \times 10^{-3}$ m) using agate mortar and pestle. Fine grains were obtained by milling these small grains in an agate vessel using a mix of agate balls ranging in size from $5–20 \times 10^{-3}$ m. A planetary mill was usually used for a period of up to 4 h. The resultant powder was graded by wet sieving through sieves ranging in size from 5–100 μm. A 6 kHz electromechanical oscillator was employed to assist the process. The liquid vehicle (ethanol) was separated using distillation and finally open evaporation.

Cold pressing was achieved using alloy steel dies and a pressure of ($30–40 \times 10^7$ N m^{-2}) which gave optimum green density. Sintering was performed in a hydrogen ambient at temperatures up to 670 K and for periods of up to 8 h.

Details of the hot pressing procedure used were given previously [11]. The dies used were TZM lined with high-purity graphite and heated by r.f. power in a vacuum furnace of 10^{-5} torr (1 torr = 1.333×10^2 Pa). Prior to heating, the powder was cold compacted using a pressure of 0.9×10^6 Pa, followed by raising the temperature to the desired value (670 K). Hot pressing was accomplished by applying a pressure of 88×10^6 Pa at a temperature of 670 K and for a period of 30 min. At the end of the 30 min the pressure was first removed, followed by switching off the r.f. power. The hot pressing was essential for obtaining a very fine powder ($L \leqslant 5$ μm) because this grain size could not be cold compacted and sintered, but using the hot-pressing procedure outlined above, density in excess of 95% single-crystal density could be obtained.

2.3. Analytical procedure

To assess the homogeneity of the resulting material, extensive use was made of metallographic techniques to reveal any precipitates. Milligram X-ray powder diffraction patterns were taken using a vertical diffractometer, employing CuK_α radiation and a graphite-diffracted beam monochromator. The values of lattice parameter [12] are very sensitive to compositional variation (Vegards law). To obtain the corrected lattice parameter values, extrapolation functions for both the c and a parameters were employed.

2.4. Electrical and thermal measurements

A d.c. four-probe technique was used throughout for the electrical resistivity measurements. Carrier concentration measurements were obtained from the Hall effect using a.c. excitation and lock-in techniques. Thermoelectric power measurements were obtained using the hot-probe technique.

Thermal conductivity measurements were made using a transient laser flash technique [13]. The heat sensor was a non-contact infrared device. The use of this sensor reduced the heat-sinking problem associated with thermocouples. The transient waveform was captured and processed under computer control. Samples of diameter 1×10^{-2} m across, lapped to a high degree of parallelism, and of thickness $1–2.5 \times 10^{-3}$ m, were used. A pulsed neodymium–glass laser of maximum output of 20 J, was used to supply the heat pulse.

3. Results and discussion

Homogeneity of these alloys was not considered to be a problem because the p-type alloy has a congruent melting point [12]; furthermore, the hot pressing achieves further homogenization [11]. Both of the alloys, whether grown by the Bridgman method or the travelling heater, produce bi- or tri-crystals across the 12 mm diameter. X-ray orientation of these crystals showed the (1 1 1) plane to be lying within 10°–15° of the freezing direction (direction of crystal axis). Bi_2Te_3-related pseudo-binary and ternary alloys have been extensively studied in single-crystal form [4, 7, 14, 15] and in powder form [16]. Their thermoelectric properties are very well characterized and this work is not intended to reestablish these properties, but rather to examine the influence of fine grain on these properties.

With this criterion in mind, two representative alloys were chosen for this study. The p-type alloy was Sb_2Te_3 rich and the n-type was Bi_2Te_3 rich. The discussion will mainly deal with the p-type alloy; for the n-type alloy, a brief mention will be made of their behaviour because it resembles that of the p-type, though not in absolute values.

3.1. p-type selenium-doped $(Bi_{0.25}–Sb_{0.75})_2Te_3$

Electrical measurement were carried out in a direction parallel to the (1 1 1) plane. An average value of electrical resistivity obtained was (0.21 Ωm) and the Seebeck coefficient was 155×10^{-6} V K^{-1}. The thermal conductivity measurements will be considered in relative terms because this is more appropriate to the comparison between single-crystal and fine-grained results of the same starting material. To establish the sintering time and temperature, a compact with ($L < 10$ μm) was sintered in a hydrogen ambient at 673 K for periods up to 6 h (Fig. 1). A maximum drop of ρ from 1.2 Ωm before sintering, to 0.5 Ωm after sintering, was achieved. Fig. 1 shows that 4 h at 673 K is about the optimum time for sintering. Fig. 2a shows

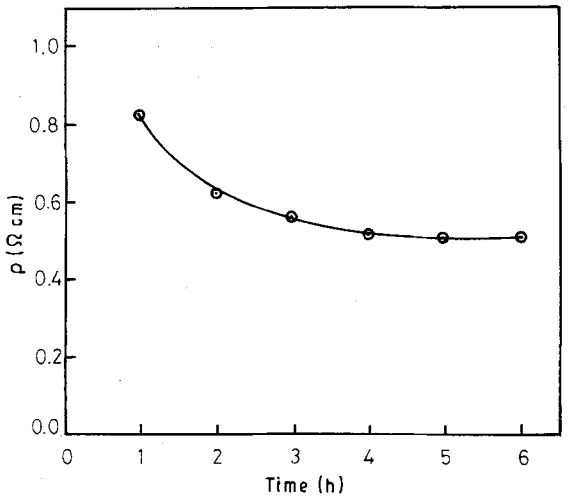

Figure 1 Variation of electrical resistivity of a compact ($L \leqslant 10$ μm), sintered at 673 K in a hydrogen ambient, with time. ρ, before sintering = 1.2 Ωm.

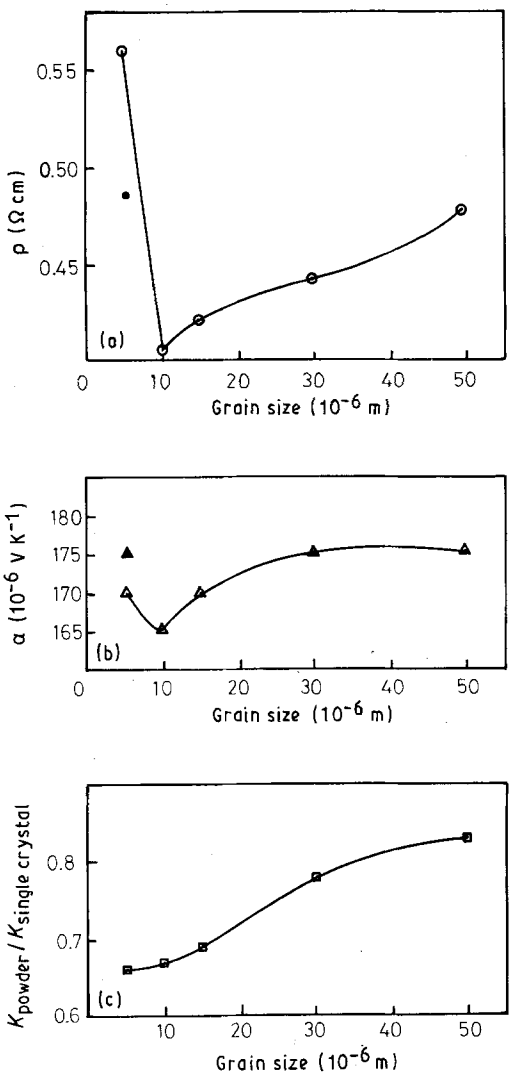

Figure 2 (a) The electrical resistivity versus grain size for p-type selenium-doped 15% Sb_2Te_3–25% Bi_2Te_3 compacts sintered at 673 K. (○) Cold pressed and sintered, (●) hot pressed. (b) The variation of Seebeck coefficient with grain size, (△) cold pressed, (▲) hot pressed. (c) The relative thermal conductivity for various grain sizes.

the electrical resistivity versus grain size for compacts sintered at 673 K. The end resistivity after sintering appears to increase with grain size and, at first sight, this appears to be contrary to expectations. If grain boundaries are assumed not to contribute to resistivity, then the grain size should not influence the resistivity and thus the end resistivity should be the same for all grain sizes. The high resistivity (0.56 Ωm) for the $L \leqslant 5$ μm grain size is due to the fact that this range of grain size could not be sintered satisfactorily via the cold pressing/sintering route due to blistering and bubble formation on the surface. This is attributed to the adsorption of gases to the large surface area of grain boundaries which coalesce during sintering to form these blisters. With the exception of $L \leqslant 5$ μm, the increase in resistivity from the single-crystal value of 0.21 Ωm to 0.404 Ωm for $L \leqslant 10$ μm is consistent with the fact that the resistivity should fall somewhere between that parallel to (1 1 1), i.e. 0.21 Ωm, and four times this value for direction perpendicular to the (1 1 1) plane, as the powder is composed of random mix of crystallites of different orientation. The higher resistivity for $L \leqslant 50$ μm than that for $L \leqslant 10$ μm is interpreted in terms of the fact that the cleavage plane in Bi_2Te_3-based alloys is parallel to the (1 1 1) plane which has the lowest resistivity, and during milling of the ingot it is expected that a larger number of crystals will find it easier to cleave parallel to the (1 1 1) plane and thus increase the probability of finding crystallites or rather flakes with surfaces parallel to the (1 1 1) plane. During pressing these flakes will pack parallel to each other and thus orientate themselves perpendicular to the pressing direction. As the larger grain compacts have fewer flakes parallel to the (1 1 1) plane, it is expected that their resistivity will be closer to the random mix powder. Conversely, the finer the grain the more flakes with the preferred orientation and thus the closer their resistivity value will be to that of the single crystal. Fig. 2b shows the variation of Seebeck coefficient with grain size and, as can be seen, the variation is marginal consistent with prediction that its value is independent of orientation. Fig. 2c shows the relative thermal conductivity for the various grain size. The variation in thermal conductivity is expected to be smaller than electrical resistivity, because the value of K parallel to (1 1 1) is only twice that perpendicular to the (1 1 1) plane. Here once again we find the relative thermal conductivity of the largest grain size ($L \leqslant 50$ μm) is larger than that for the fine grain, and this is consistent with the probability of finding (1 1 1) planes. The fact that the relative value of K for the finest grain is smaller than that for single crystal is attributed to two processes operating; the first is that due to flakes packing parallel to the (1 1 1) plane and thus retaining some of the single crystal feature, and the second is due to phonon/grain-boundary scattering.

Fig. 3 shows the figure of merit for the various grain size. Contrary to expectations, $L \leqslant 5$ μm shows very low value of Z and this is caused by the high resistivity value caused by blistering. To overcome this the powder with grain size $L \leqslant 5$ μm was hot pressed. The effect of hot pressing was to bring down the resistivity

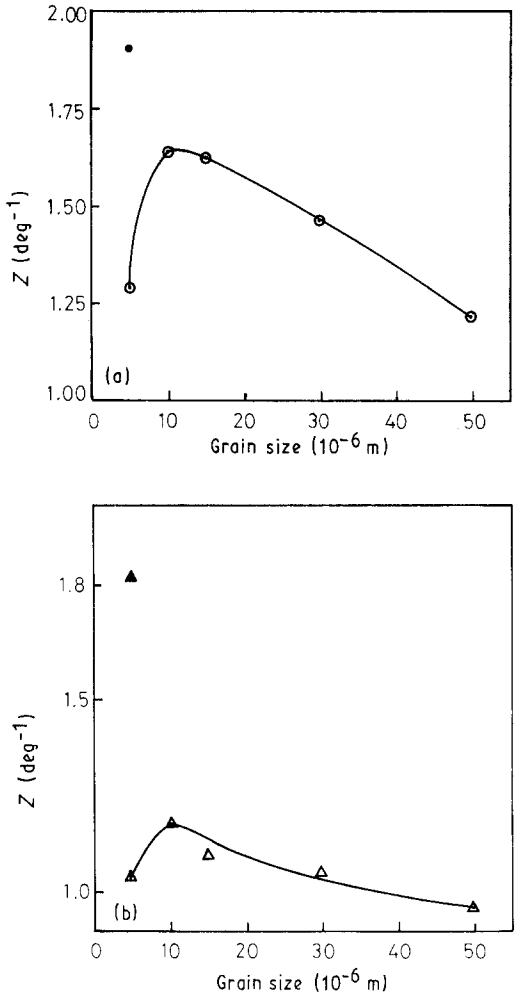

Figure 3 Variation of the figure of merit, Z, with grain size for (a) p- and (b) n-type selenium-doped 75% Sb_2Te_3–25% Bi_2Te_3. (●, ▲) Hot pressed, (○, △) cold pressed. $Z_{\text{single crystal}} = 1.87\,K^{-1}$.

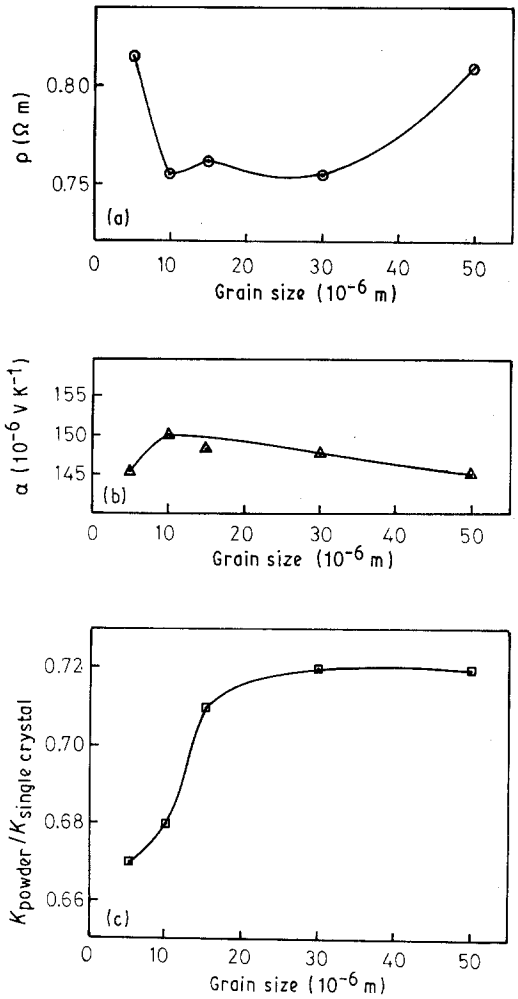

Figure 4 Variation of (a) the electrical resistivity, ρ, (b) the Seebeck coefficient, α, and (c) the relative thermal conductivity with grain size of n-type SbI_3-doped 90% Bi_2Te_3–5% Sb_2Te_3–5% Sb_2Se_3 alloy. $\rho_{\text{hot pressed}} = 0.445\,\Omega m$, $\alpha_{\text{hot pressed}} = 142 \times 10^{-6}\,V\,K^{-1}$.

to a value of 0.475 Ωm compared with 0.5 Ωm obtained from cold pressing. The Seebeck coefficient is now closer to the value of the coarser grains (170 $\times 10^{-6}\,V\,K^{-1}$). The relative thermal conductivity of the hot-pressed powder represents a drop of some 45%, brought about by a combination of two processes, the phonon scattering at grain boundaries and the flake packing parallel to the (1 1 1) plane.

3.2. n-type alloy SbI_3-doped 90% Bi_2Te_3–5% Sb_2Te_3–5%Sb_2Se_3

Fig. 4 shows the electrical and thermal measurements. As can be seen the general behaviour closely resembles that for the p-type alloy except for the relative thermal conductivity for the hot-pressed material which is identical to that for the cold-pressed and sintered sample for the $L \leqslant 5$ μm size. The hot pressing appears to have influenced the electrical resistivity to a larger extent, i.e. the resistivity of the cold pressed $L \leqslant 5$ μm sample dropped from a resistivity value of 0.81 Ωm to 0.445 Ωm when hot pressed. The drop in thermal conductivity of the finest grain ($L \leqslant 5$ μm) of the hot-pressed or cold-pressed n-type is some 37%, and this is once again brought about by the combination of the grain-boundary/phonon scattering and flake packing

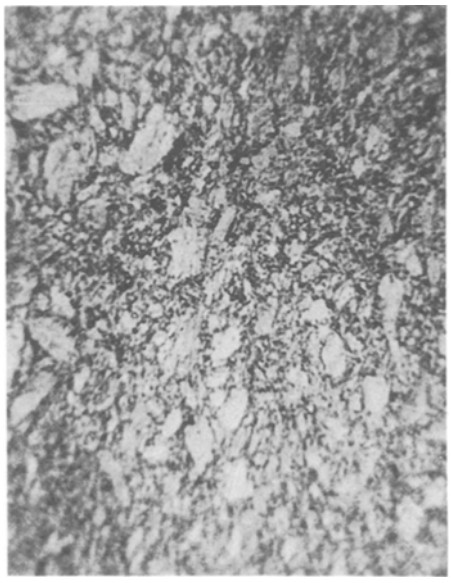

Figure 5 Grain structure of p-type hot-pressed alloy, $L \leqslant 5$ μm, ×1150.

or layering that retains some of the anisotropy of the single crystal.

From Fig. 3, it appears that for the finest grain size ($L \leqslant 5$μm), the figure of merit for the p-type is almost

equal to that of the single crystal, while that for the n-type is some 90% of it. The figure of merit for these single-crystal alloys agrees closely with those reported elsewhere [7] for alloys of similar resistivity. This work does not lend support to the work of Ryden [16], which is to be expected in view of the fact that in his treatment, Ryden assumes that packing of the powder is random. A full treatment should consider the effect of the size of the grain when it is comparable to the wavelength of the scattered wave. Scattering of phonons in these alloys by small grains is attributable to the fact that the grains at the lower grain-size range used in these experiments became comparable to the effective phonon mean free path. The recent work of Schreiner [17] reports similar results to this work for a p-type alloy of different resistivity, 70% Sb_2Te_3–30% Bi_2Te_3, i.e. for an alloy of 0.084 Ωm, Z is given to be 2.75 K^{-1}, which is almost 100% of the Z value reported by Yim and Rosi [7] for single crystal. A typical hot-pressed grain structure is shown in Fig. 5.

Acknowledgement

The authors thank the King Abdul Aziz City for Science and Technology for the use of some of the research facilities that were provided under project AT-4-42.

References

1. H. J. GOLDSMID and R. W. DOUGLAS, *Brit. J. Appl. Phys.* **5** (1954) 386.
2. A. F. IOFFE, "Semiconductor Thermoelements and Thermoelectric Cooling", English edition (Infosearch, London, 1957).
3. U. BIRKHOLZ, *Z. Naturforsch.* **13a** (1958) 780.
4. F. D. ROSI, B. ABELES and R. V. JENSEN, *J. Phys. Chem. Solids* **10** (1959) 191.
5. K. SMIROUS and L. STOURAC, *Z. Naturforsch.* **14a** (1959) 848.
6. F. D. ROSI, E. F. HOCKINGS and N. E. LINDENBLAD, *R.C.A. Rev.* **22** (1961) 82.
7. W. M. YIM and F. D. ROSI, *Solid State Electron.* **15** (1972) 1121.
8. W. M. YIM, E. V. FITZKE and F. D. ROSI, *J. Mater. Sci.* **1** (1966) 52.
9. R. R. HEIKES and R. W. URE Jr, "Thermoelectricity Science and Engineering" (Interscience, New York, 1961).
10. D. M. ROWE, *J. Phys. D* **7** (1974) 1843.
11. F. A. A. AMIN, M. A. A. ISSA, A. M. HASSIB and Z. H. DUGHAISH, *J. Mater. Sci.* **20** (1985) 4130.
12. M. J. SMITH, R. J. KNIGHT and C. W. SPENCER, *J. Appl. Phys.* **33** (7) (1962) 2186.
13. Final Report of Research Project AT-4-42, King Abdulaziz City for Science and Technology (1986).
14. U. BIRKHOLZ, *Z. Naturforsch.* **13a** (1958) 78.
15. H. J. GOLDSMID, *J. Appl. Phys.* **32** (1961) 2198.
16. D. J. RYDEN, *J. Phys. C Solid State Phys.* **4** (1971) 1193.
17. H. SCHREINER, *Powder Metall. Int.* **17** (4) (1985) 195.

Received 27 November 1990
and accepted 10 April 1991